The Astrophysical Journal, 771:63 (11pp), 2013 July 1 doi:10.1088/0004-637X/771/1/63

NUCLEAR ACTIVITY IS MORE PREVALENT IN STAR-FORMING GALAXIES

D. J. Rosario[1], P. Santini[2], D. Lutz[1], H. Netzer[3], F. E. Bauer[4,5], S. Berta[1], B. Magnelli[6], P. Popesso[1], D. M. Alexander[7], W. N. Brandt[8], R. Genzel[1], R. Maiolino[9,10], J. R. Mullaney[7], R. Nordon[3], A. Saintonge[1], L. Tacconi[1], and S. Wuyts[1]
[1] Max-Planck-Institut für Extraterrestrische Physik (MPE), Postfach 1312, D-85741 Garching, Germany; rosario@mpe.mpg.de, lutz@mpe.mpg.de, berta@mpe.mpg.de, popesso@mpe.mpg.de, genzel@mpe.mpg.de, amelie@mpe.mpg.de, linda@mpe.mpg.de, swuyts@mpe.mpg.de
[2] INAF-Osservatorio Astronomico di Roma, via di Frascati 33, I-00040 Monte Porzio Catone, Italy; paola.santini@oa-roma.inaf.it
[3] School of Physics & Astronomy, Tel Aviv University, 69978 Tel Aviv, Israel; netzer@wise.tau.ac.il, nordon@astro.tau.ac.il
[4] Departamento de Astronomía y Astrofísica, Pontificia Universidad Católica de Chile, Casilla 306, Santiago 22, Chile; fbauer@astro.puc.cl
[5] Space Science Institute, 4750 Walnut Street, Suite 205, Boulder, CO 80301, USA
[6] Argelander-Institut für Astronomie, Auf dem Hügel 71, D-53121 Bonn, Germany; magnelli@astro.uni-bonn.de
[7] Department of Physics, Durham University, South Road, Durham, DH1 3LE, UK; d.m.alexander@dur.ac.uk, j.r.mullaney@durham.ac.uk
[8] Department of Astronomy & Astrophysics, 525 Davey Lab, The Pennsylvania State University, University Park, Pennsylvania, PA 16802 USA; niel@astro.psu.edu
[9] Kavli Institute for Cosmology, University of Cambridge, Madingley Road, Cambridge CB3 OHA, UK; r.maiolino@mrao.cam.ac.uk
[10] Cavendish Laboratory, University of Cambridge, 19 JJ Thomson Avenue, Cambridge, CB3 OHE, UK
Received 2012 December 14; accepted 2013 May 12; published 2013 June 17

ABSTRACT

We explore the question of whether low and moderate luminosity active galactic nuclei (AGNs) are preferentially found in galaxies that are undergoing a transition from active star formation (SF) to quiescence. This notion has been suggested by studies of the UV–optical colors of AGN hosts, which find them to be common among galaxies in the so-called Green Valley, a region of galaxy color space believed to be composed mostly of galaxies undergoing SF quenching. Combining the deepest current X-ray and *Herschel*/PACS far-infrared (FIR) observations of the two Chandra Deep Fields with redshifts, stellar masses, and rest-frame photometry derived from the extensive and uniform multi-wavelength data in these fields, we compare the rest-frame $U - V$ color distributions and star formation rate distributions of AGNs and carefully constructed samples of inactive control galaxies. The UV-to-optical colors of AGNs are consistent with equally massive inactive galaxies at redshifts out to $z \sim 2$, but we show that such colors are poor tracers of SF. While the FIR distributions of both star-forming AGNs and star-forming inactive galaxies are statistically similar, we show that AGNs are preferentially found in star-forming host galaxies, or, in other words, AGNs are *less* likely to be found in weakly star-forming or quenched galaxies. We postulate that, among X-ray-selected AGNs of low and moderate accretion luminosities, the supply of cold gas primarily determines the accretion rate distribution of the nuclear black holes.

Key words: galaxies: active – galaxies: evolution – galaxies: star formation – infrared: galaxies – surveys – X-rays: galaxies

Online-only material: color figures

1. INTRODUCTION

Accreting black holes are arguably the most efficient engines of energy production in the universe. The deep gravitational wells of supermassive black holes (SMBHs) allow the extraction of ∼10% of the rest mass energy of the material that falls into their horizons, which, through accretion processes, is ultimately converted into the electromagnetic and mechanical output that power active galactic nuclei (AGNs). This energy can, in turn, escape into the environs of the AGN host galaxy, affecting material on large scales. Such AGN "feedback" has many potential effects on galaxy physics and evolution: regulation of the circumnuclear environment and galactic star formation (SF), gaseous outflows, the distribution of metals, enrichment and heating of gas in the circumgalactic medium. There is much observational evidence for the direct effects of SMBH activity on their host galaxies, either in the form of AGN-driven outflows (Holt et al. 2008; Alexander et al. 2010; Feruglio et al. 2010; Fischer et al. 2010; Greene et al. 2011; Rupke & Veilleux 2011; Sturm et al. 2011; Cano-Díaz et al. 2012; Harrison et al. 2012b; Maiolino et al. 2012) or bubbles blown in the host atmospheres of massive galaxy halos by powerful radio jets (McNamara & Nulsen 2007; Gitti et al. 2012).

Proposed evidence for the widespread action of SMBH feedback on the SF histories of galaxies comes from suggestions that most AGNs occupy a preferred population of host galaxies, those that are undergoing a transformation from active steady SF to a final state of quiescence (e.g., Nandra et al. 2007; Martin et al. 2007; Schawinski et al. 2010). These two phases form the basis of the well-known color bimodality of galaxies—most galaxies from the local universe to $z \sim 3$ lie in two relatively distinct parts of the color–magnitude or color–mass diagram (CMD), the blue cloud and the red sequence. Galaxies that lie at intermediate colors on these diagrams are believed to be transitioning between the two populations, through a region known as the "Green Valley (GV)" (e.g., Faber et al. 2007). The preponderance of GV galaxies among AGN hosts has been taken as evidence that low-to-moderate luminosity AGNs are responsible for the quenching of SF in galaxies, mediated through feedback from the SMBH. The closely associated morphological evolution of transforming galaxies (Driver et al. 2006; Kauffmann et al. 2006; Franx et al. 2008; Cheung et al. 2012) is taken to be evidence that a substantial fraction of AGNs are related to, and perhaps triggered by, galaxy mergers which may be responsible for the formation of "red and dead" ellipticals.

In recent work, the notion that AGNs prefer quenching hosts has come under greater scrutiny. The importance of stellar mass selection effects for the interpretation of AGN colors seems to suggest that AGN host colors are not radically different from

similarly massive inactive galaxies (Xue et al. 2010; Rosario et al. 2013). A previous study by our team (Santini et al. 2012b) found that mean star formation rates (SFRs) are enhanced in X-ray AGNs over inactive galaxies of the same stellar mass, with tentative evidence that the enhancement was caused by a lower fraction of quiescent galaxies among AGN hosts, rather than a boost in the SFRs of star-forming AGNs. However, given the relatively shallow far-infrared (FIR) data used in this earlier work, this notion could not be tested extensively.

In this paper, we critically examine the evidence that AGNs are preferentially in galaxies that are quenching or undergoing a slowdown of their global SF. Rather than relying only on optical or UV tracers of SF such as the CMD, we employ instead the most sensitive FIR data currently available from the *Herschel Space Telescope*, together with a large sample of AGNs selected from the deepest extragalactic X-ray surveys on the sky—the two Chandra Deep Fields (CDFs). In Section 2, we present the surveys, selection, and data sets. In Section 3, we compare the use of FIR tracers and UV–optical colors in studies of SF. In Sections 4 and 5, we re-examine the evidence that AGNs lie preferentially in the GV, then fold in information about the FIR luminosities and detection rates of AGNs toward exploring the question of whether AGNs are in quenching galaxies. Our results are discussed in Section 6. In this work, we assume a Λ-CDM concordance cosmology with $\Omega_\Lambda = 0.7$, $\Omega_m = 0.3$, and $H_0 = 70$ km s^{-1}Mpc^{-1}.

2. DATA SETS AND SAMPLE SELECTION

2.1. Sample Selection and Data Sets

Cospatial with the two GOODS survey fields (Giavalisco et al. 2004), the CDFs are the deepest pencil-beam X-ray surveys in the sky. In GOODS-North, the CDF-North X-ray catalog comprises 503 sources from a total exposure of 2 Ms (Alexander et al. 2003), while in GOODS-South, the new 4 Ms CDF-South X-ray catalog consists of 740 sources (Xue et al. 2011). We have extensively characterized the data and catalogs in both fields, in which careful associations have been made with optical and near-IR counterparts, using, where possible, probabilistic cross-matching models (Luo et al. 2010; Xue et al. 2011). In addition to the deep X-ray data, the wealth of deep spectroscopy and multi-wavelength photometric data in the GOODS fields have enabled accurate spectroscopic or AGN-optimized photometric redshifts to be determined for the majority of the X-ray sources (e.g., Szokoly et al. 2004; Luo et al. 2010). We estimate absorption-corrected hard-band X-ray luminosities (L_X) of sources with redshifts using spectral modeling techniques (Bauer et al. 2004). As a result of the small area and great depth of the CDF exposures, most X-ray sources are low or moderate luminosity AGNs—only $\sim$5% of the sources have $\log L_X(2\text{–}10\ \mathrm{keV}) > 44$ erg s^{-1}. These have equivalent AGN bolometric luminosities to the Seyfert galaxy population found in the local universe. In this work, we only consider sources with $\log L_X > 42$ erg s^{-1}to prevent contamination from powerful starbursts, in which emission from X-ray binaries can potentially overpower the emission from nuclear activity in such faint systems.

We employ multiwavelength galaxy catalogs for the two GOODS fields to define a general galaxy sample, the properties of which we will compare to the AGNs. In GOODS-S, we use the updated GOODS-MUSIC database (Santini et al. 2009; Grazian et al. 2006), while in GOODS-N we use a catalog developed for the PEP team using similar methodologies (Berta et al. 2010, 2011).[11] The former catalog selects galaxies with observed magnitudes in the *Hubble Space Telescope* F850LP band <26 or in the ISAAC K_s band <23.5, while the latter is primarily selected to have $K < 24.2$. In order to exclude a surfeit of faint sources with inaccurately red colors and masses, we apply an additional cut of F850LP < 26 in the GOODS-N catalog. For galaxies with no current spectroscopic redshifts, photometric redshifts were determined by fitting multiwavelength photometry using PEGASE 2.0 templates (Fioc & Rocca-Volmerange 1997) in GOODS-S or using the EAZY code (Brammer et al. 2008) in GOODS-N. For details on the catalog preparation, characterization, and photometric redshift estimation, we refer the reader to Santini et al. (2009) and Berta et al. (2010) for GOODS-S and GOODS-N, respectively.

While AGNs are selected by their X-ray emission, we define our "inactive" galaxy population as all galaxies that are undetected in X-rays (excluding even those which have $\log L_X < 42$ erg s^{-1}) and with mid-IR (MIR) colors (i.e., based on *Spitzer*/IRAC photometry) that do not satisfy the AGNs selection criteria of Donley et al. (2012). In practice, only a very small fraction of the general galaxy population are rejected on the basis of these criteria. These rejected objects, however, tend to be in massive galaxies and could potentially sway the statistics of SF comparisons among such systems by an inordinate degree.

We have developed a custom technique for the estimation of stellar masses (M_*) in AGNs by linearly combining galaxy population synthesis model templates and AGNs spectral energy distribution (SED) templates to fit multiwavelength photometry. For inactive galaxies, we perform a χ^2 minimization of Bruzual & Charlot (2003) synthetic models, assuming a Salpeter initial mass function (IMF) and parameterizing the SF histories as exponentially declining laws. For AGNs, we also include an AGN template from Silva et al. (2004), which accounts for a variable fraction of the total light of the galaxy. The AGN template reflects the classification of the X-ray source, derived from information about its SED and spectrum, where available. For sources classified as Type I (broad lines in the spectrum, clear AGN contribution in the rest-frame optical and UV), a Seyfert 1 SED was used, while for the rest, a Seyfert 2 template was used if the estimated X-ray absorption column $N_{\mathrm{H}} < 10^{24}$ cm^{-2}, and a Compton-thick template for more heavily absorbed systems. For further details, performance evaluations and tests of the method, we refer the reader to Santini et al. (2012b).

Our FIR data are composed of maps at 70 μm, 100 μm, and 160 μm from a combination of two large *Herschel*/PACS programs: the PACS Evolutionary Probe (PEP), a guaranteed time program (Lutz et al. 2011) and the GOODS-*Herschel* key program (Elbaz et al. 2011). The combined PEP+GH (PEP/GOODS-*Herschel*) reductions are described in detail in B. Magnelli et al. (2013). While data at 100 and 160 μm are available in both fields, an additional deep map at 70 μm is also available in GOODS-S. The PACS 160, 100, and 70 μm fluxes were extracted using sources from archival deep *Spitzer* MIPS 24 μm catalogs as priors, following the method described in Magnelli et al. (2009); see also Lutz et al. (2011) for more details. 3σ depths are 0.90/0.54/1.29 mJy at 70/100/160 μm in the central region of GOODS-S and 0.93/2.04 mJy at 100/160 μm in GOODS-N. The GOODS-S maps are $\approx$80% deeper

[11] Available on the PEP public release page.

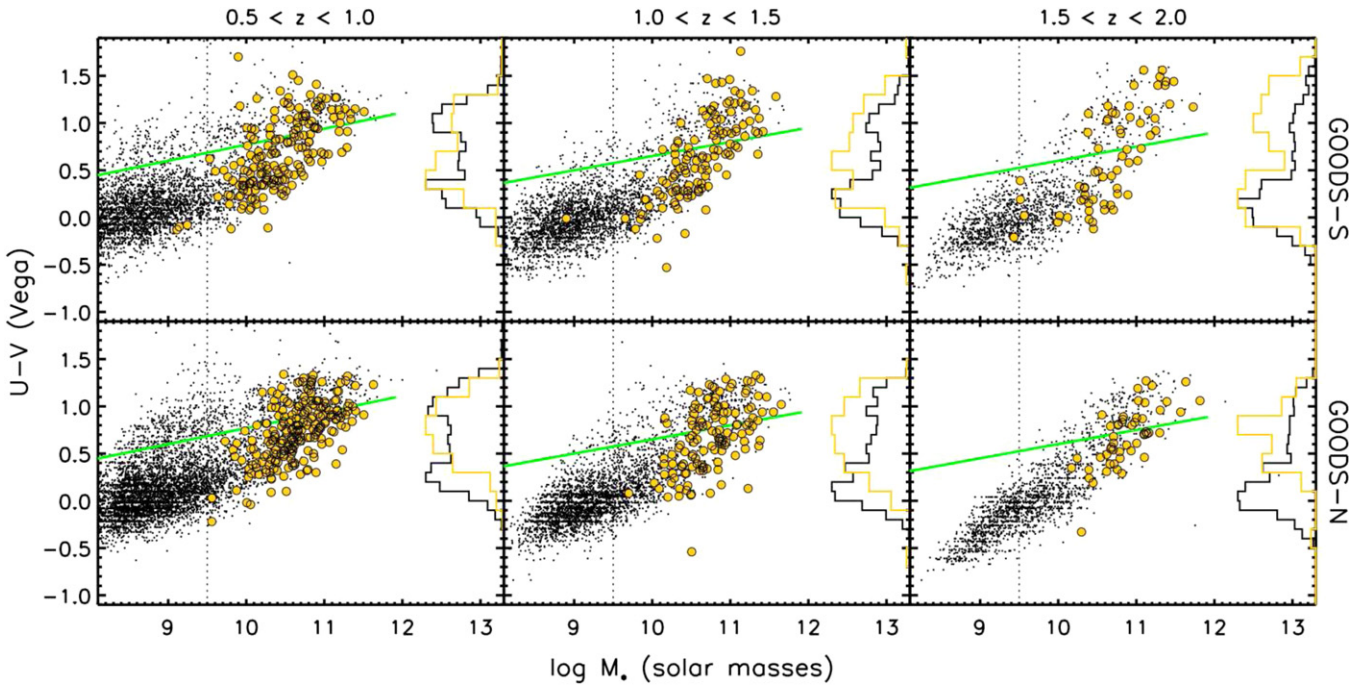

Figure 1. Color–mass diagrams (CMDs) of rest-frame $U - V$ color against stellar mass (M_*). All X-ray sources and IRAC-selected AGNs have been excluded from these diagrams. The general galaxy population taken from the full galaxy catalogs in both GOODS fields are shown as small black points, with the distribution of $U - V$ color for galaxies with $M_* > 10^{9.5}\ M_\odot$ (dotted line) shown as a black histogram on the right axis of each panel. A color bimodality is seen at all redshifts. The location of the "Green Valley" is shown by solid green lines which mark the locus of minimum galaxy density in this diagram (see Section 3 and Table 1). FIR-detected galaxies (for a definition, see Section 2) are shown as large colored points and their $U - V$ distribution is shown on the right axis of each panel as a colored histogram. Both histograms are normalized to have the same peak value. Despite lying on or above the SF mass sequence, most FIR-detected galaxies exhibit $U - V$ colors that are intermediate between the red and blue sequences, i.e., they lie in the Green Valley and show a weak color bimodality. This is primarily because of their high stellar masses.

(A color version of this figure is available in the online journal.)

than the GOODS-N maps and probe further down the FIR luminosity function at all redshifts (B. Magnelli et al. 2013).

For practical purposes, we use the monochromatic luminosity of a galaxy at 60 μm rest (L_{60}) as a measure of its FIR luminosity. The PACS bands cover this rest-frame wavelength over much of the redshift range probed in this work and we estimate L_{60} from a simple log-linear interpolation of PACS measurements in bands that bracket 60 μm in the rest frame. The use of L_{60} obviates the need to apply an uncertain correction between monochromatic and total FIR luminosities. Nevertheless, in order to relate L_{60} to the properties of the population of star-forming galaxies from the existing literature, such as the SF "mass sequence" or "main sequence" (MS), we adopt the following relationship between L_{60} and SFR:

$$L_{\rm IR} = f_{CE01} \times L_{60} \quad (1)$$

$$\mathrm{SFR} = 1.72 \times 10^{-10} L_{\rm IR}. \quad (2)$$

f_{CE01} is the conversion factor between L_{60} and the total IR luminosity integrated over 8–1000 μm ($L_{\rm IR}$) from Chary & Elbaz (2001). This factor is IR luminosity dependent, but only varies slightly over the range 1.6–2.5. The conversion factor between SFR and $L_{\rm IR}$ is taken from Kennicutt (1998), which also assumes a Saltpeter IMF.

3. THE COLORS AND MASSES OF FIR-DETECTED INACTIVE GALAXIES

We begin by first examining the relationship between the optical color of galaxies and the SFR or SF luminosity, as traced by FIR emission. For this, we turn to the CMD as a diagnostic tool. In Figure 1, we plot the rest-frame $U - V$ color against the stellar mass M_* of galaxies, separately for the two GOODS fields. Consistent with several previous studies in these and other extragalactic fields (e.g., Willmer et al. 2006; Wyder et al. 2007; Taylor et al. 2009; Brammer et al. 2009; Whitaker et al. 2011), galaxies tend to cluster in two well-defined regions of the diagram: the red sequence and the blue cloud. These structures form the basis of the well-known color bimodality of galaxies, which has been revealed to $z > 2$ (Brammer et al. 2009). In such optical- or NIR-selected photometric catalogs, the mass limit, revealed by the sharp boundary in the density of galaxies at the lower mass end of the diagram, is redshift and color dependent. At $z > 1.5$, the mass limit is high enough among red galaxies that it blurs the definition of the color bimodality. In addition, at these redshifts, a population of extremely dust-reddened galaxies is also seen, leading to a tail of very red colors among high-mass galaxies.

In between the dense red sequence and blue cloud, galaxies have intermediate colors, which has led to the popular name for this area of the CMD: the GV. Taking the GV as a minimum in the density distribution of galaxies on the CMD at a given stellar mass, we construct sloped lines on the CMD which separate the red sequence from the blue cloud and define the location of the GV for all our subsequent analysis. The slope and normalization of the lines were determined by eye to yield the most well-defined separation between the red sequence and blue cloud in each redshift bin. We tabulate the GV lines for each bin in Table 1 and plot them in Figure 1 using solid green lines.

It has been suggested, based on the low density of the GV, that most galaxies here are going through a relatively rapid phase of SF quenching, resulting in a net flow of galaxies from

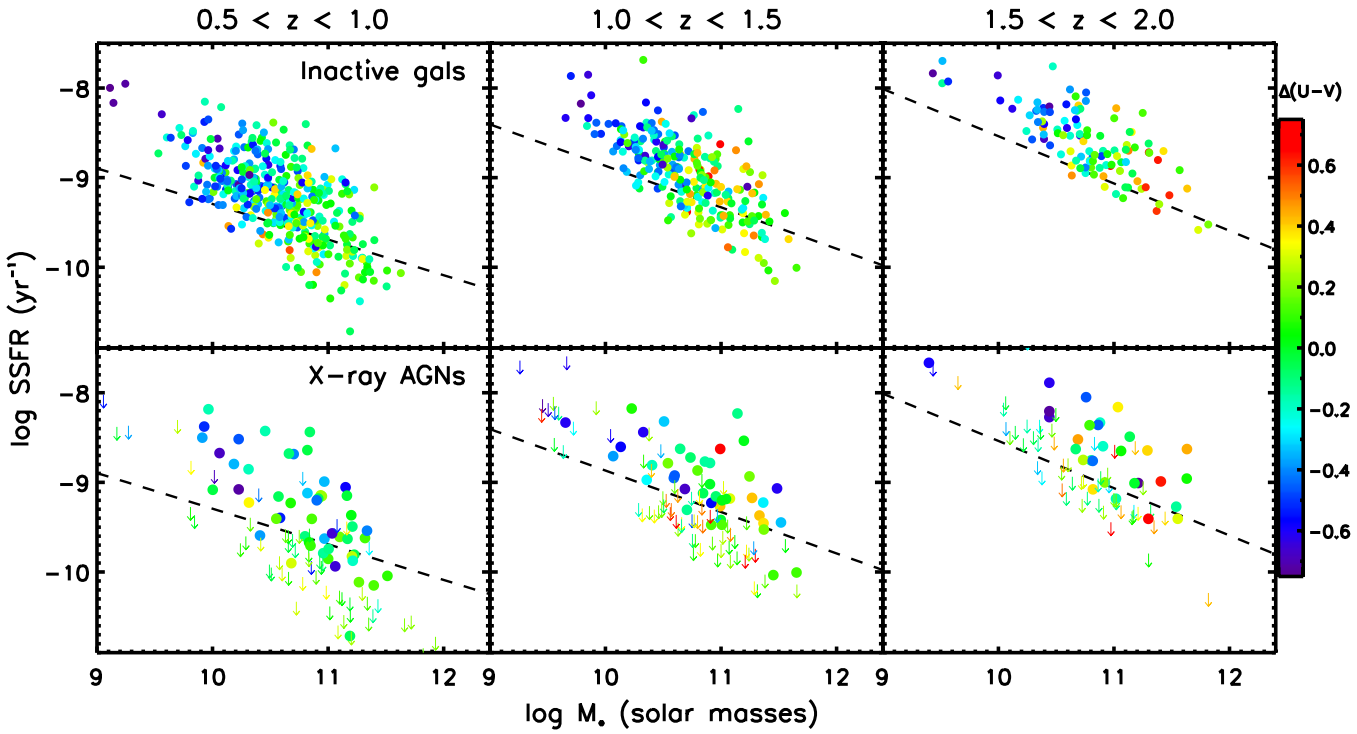

Figure 2. Specific star formation rate (SSFR) against stellar mass (M_*) of PACS-detected inactive galaxies (top panels) and X-ray-selected AGNs (bottom panels). For AGNs undetected in PACS, we also show estimated upper limits on SSFR (arrow points). Points are colored by the $\Delta(U-V)$, the $U-V$ offset of the galaxy from the Green Valley (GV) as defined by straight lines in the CMD (Section 3). Galaxies that lie in the GV have $\Delta(U-V)$ close to zero and are colored as green points in the figure. Both PACS-detected galaxies and PACS-detected AGNs in the GV lie on or around the mass sequence (shown as dashed lines) and are typically massive, while those in the blue cloud are typically at lower masses and lie well above the mass sequence. A substantial fraction of objects in the GV are normal massive SF galaxies at all redshifts in this study. The distribution of both PACS-detected AGNs and inactive galaxies about the mass sequence are formally indistinguishable, as developed further in Section 5.

(A color version of this figure is available in the online journal.)

Table 1
Parameters of the Green Valley (GV) Lines in the Color–Mass Diagram

Redshift Interval	UV_9	α
0.5–1.0	0.60	0.17
1.0–1.5	0.50	0.15
1.5–2.0	0.45	0.15

Notes. UV_9 and α are defined such that $(U-V)_{\rm GV} = \alpha \log(M_{*,9}) + UV_9$, where $(U-V)_{\rm GV}$ is the color of the GV line and $M_{*,9}$ is the stellar mass in units of 10^9 solar masses.

the SF blue cloud to the quiescent red sequence (Faber et al. 2007; Martin et al. 2007; Brammer et al. 2011). In other words, GV galaxies are believed to have lower specific SFRs (SSFRs) compared to normal SF galaxies, which are defined to lie on the SF mass sequence (Noeske et al. 2007; Elbaz et al. 2007; Santini et al. 2009; Rodighiero et al. 2011; Wuyts et al. 2011; Whitaker et al. 2012).

Figure 1 suggests otherwise. We have plotted in this figure, using large colored symbols, the locations of PACS-detected inactive galaxies from the PEP+GH catalogs. In general, these galaxies lie on or above the MS at $z > 0.5$ and tend to be rather massive ($M_* \gtrsim 10^{10}\ M_\odot$). It is clear from the plot that a substantial, number of FIR-bright galaxies lie in the GV. In fact, the main determinant of whether or not a galaxy is detected in PACS is its stellar mass, not its color.

This can be examined in a different way using Figure 2, where we have plotted the FIR-derived SSFR of PACS-detected inactive galaxies against M_* (upper panels). The ridgeline of the SF MS at the central redshift of each redshift bin is shown in these plots as dashed lines, as determined recently by Whitaker et al. (2012). The points here are colored by $\Delta(U-V)$, the $U-V$ color offset of the galaxy from the GV in the CMD, i.e., the vertical offset of the galaxy from the green GV lines in Figure 1.

The steeper slope of the PACS-detected galaxies compared to the MS lines is due to the flux limit of the PACS photometry, which translates into a mass-dependent limit in SSFRs at a given redshift. At lower M_*, only galaxies that lie at progressively higher SFRs above the MS are detectable in PEP+GH. This strongly affects the interpretation of the slope of the MS purely from FIR data, which is why we adopt MS relationships determined, in this case, from a uniform study of deeper UV and 24 μm photometry (Whitaker et al. 2012). We have changed the mass scaling in the relations of Whitaker et al. (2012), estimated using a Chabrier IMF, upward by a factor of 1.74 to reflect our use of the Salpeter IMF (Santini et al. 2012a).

At $M_* > 10^{10.5}\ M_\odot$, we see that galaxies that lie around the MS have colors that are typical of the GV, i.e., with $\Delta(U-V) \approx 0$ (see also Whitaker et al. 2012; Salmi et al. 2012). In essence, this means that massive galaxies with intermediate colors are not a special population that is quenching and moving away from a state of ongoing SF, but, indeed, *are* the star-forming population at $M_* \gtrsim 10^{10.5}\ M_\odot$.

In later sections, we examine the PACS detection fractions of AGNs and inactive galaxies. It is worthwhile, at this stage, to note that PACS-detected galaxies primarily lie on or above the MS, even though the MS is known to have a roughly symmetrical scatter of about 0.3 dex in SSFRs (Noeske et al.

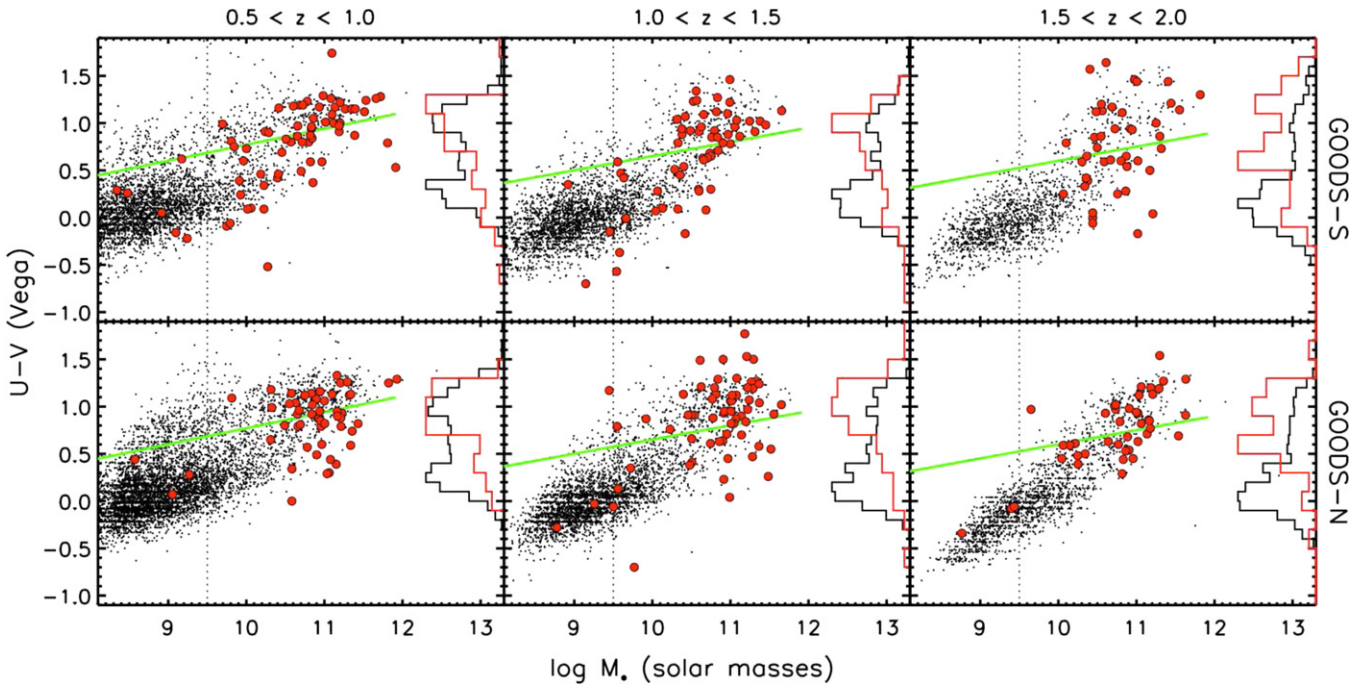

Figure 3. Color–mass diagrams (CMDs) of rest-frame $U - V$ color against stellar mass (M_*) comparing AGNs and inactive galaxies. The general galaxy population of inactive galaxies are shown as small black points, with the distribution of $U - V$ color for galaxies with $M_* > 10^{9.5}\ M_\odot$ (dotted line) shown as a black histogram on the right axis of each panel. X-ray-selected AGNs are shown as large colored points and their $U - V$ distribution is shown on the right axis of each panel as a colored histogram. Both histograms are normalized to have the same peak value. The location of the "Green Valley" is shown by solid green lines as in Figure 1. AGNs exhibit typically high stellar masses, similar to FIR-detected star-forming galaxies (compare this plot to Figure 1).

(A color version of this figure is available in the online journal.)

2007; Rodighiero et al. 2011). Concentrating only on PACS-detected galaxies restricts us to galaxies that scatter above the MS, but one must remember that there are normal star-forming galaxies that nominally lie within the MS but are below our detection limit since they lie within the scatter below the MS. When discussing PACS detection statistics, we lump together quiescent and quenching galaxies, which are expected to lie well below the normal scatter of the MS, and "weakly SF galaxies," those that lie in the low scatter of the MS. The reader should keep in mind that the population of PACS-undetected galaxies are not all quiescent or quenching, but will in addition include a sizable number of actively SF galaxies that are simply below our nominal PACS detection limits.

4. THE COLORS OF X-RAY AGNs: COMPARISON TO INACTIVE GALAXIES

We have shown the rest-frame optical color is not an ideal tracer to identify a quenching population because its use as a measure of the SF properties of a galaxy depends on the stellar mass of the galaxy. Nevertheless, several previous studies have taken the location of AGNs in the CMD as evidence for a link between AGN activity and the transformation of galaxies (e.g., Nandra et al. 2007; Martin et al. 2007; Schawinski et al. 2010). The reason for this can be seen in Figure 3. The AGNs, shown as large colored points, scatter mostly about the GV lines that we defined in Section 3, with a small scatter to lower masses and colors in the blue cloud. In many ways, the approximate distribution of AGNs in the CMD mirrors that of PACS-detected inactive galaxies. However, this is almost completely because both AGNs and FIR-bright galaxies are typically quite massive.

Indeed, it is this strong tendency for X-ray-detected AGNs to lie in massive host galaxies that mostly determines the location of the AGNs in the CMD. Recent studies suggest that, once the particular mass distribution of AGN hosts is taken into account, the colors of AGNs and inactive galaxies are very similar (Silverman et al. 2009; Xue et al. 2010; Cardamone et al. 2010; Rosario et al. 2013). The small sizes of AGN samples, generally only a few percent of galaxies, make it difficult to identify statistically robust differences in the colors of AGNs and inactive galaxies. Here, we develop a method that builds on the much larger sample of inactive galaxies to test the following null hypothesis: AGN hosts are drawn randomly from the population of massive galaxies and share the SFRs and colors of the parent sample.

For each AGN, we choose, at random and allowing duplicates, an inactive galaxy in the same redshift bin and with a stellar mass within ± 0.1 dex of the mass of the AGN host galaxy. In this way, we arrive at a sample of inactive galaxies which are equal in number and mass distribution as the AGNs in the redshift bin. The mass tolerance is smaller than the typical error in stellar masses from our SED fits, ensuring essentially identical mass distributions of AGNs and inactive galaxies. From this comparison sample, we derive a distribution in color. We repeat this process for a total of 1000 trials. This bootstrap approach gives us the typical uncertainty in the color distribution for inactive galaxies that share the mass distribution of AGNs.

In Figure 4, we compare $\Delta(U - V)$, the $U - V$ color offset from the GV, of AGNs and inactive galaxies. The distribution of $\Delta(U - V)$ for the AGNs are shown as an open histogram, plotted over the distributions of an equal number of inactive galaxies with the same redshift and stellar mass range as the AGNs. Using our bootstrap procedure, we obtain 1σ and 2σ uncertainties on the inactive galaxy distributions, shown as dark and light gray shaded regions in the figure. The colors of AGNs are statistically different from those of the inactive galaxies only

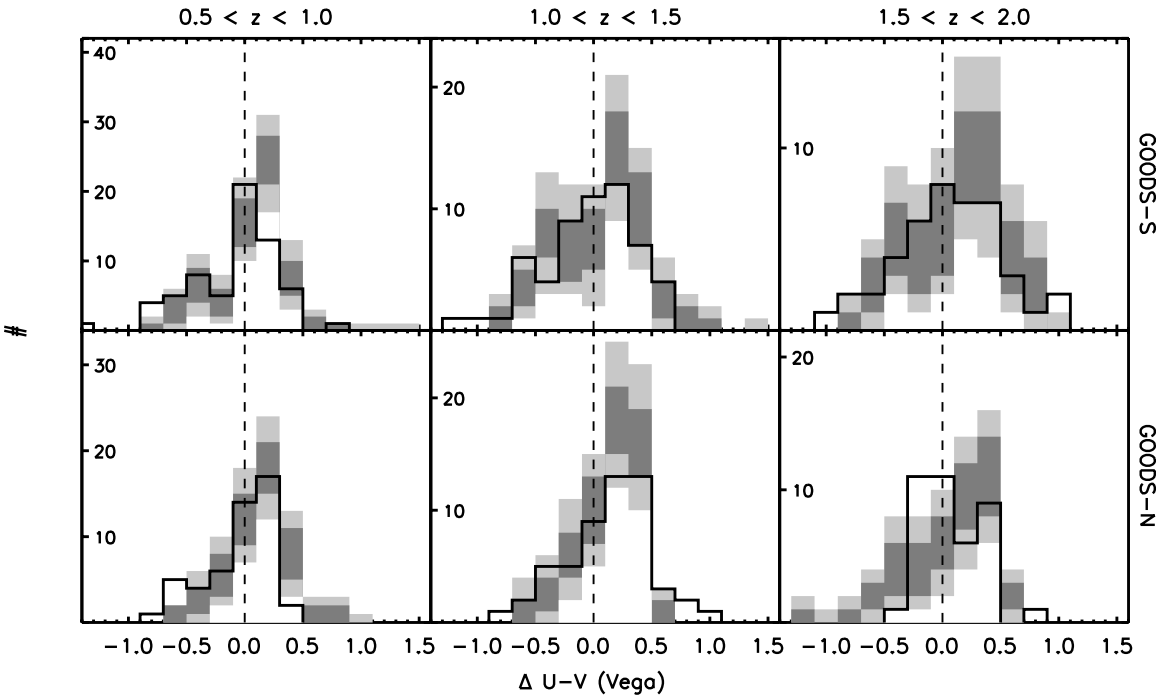

Figure 4. Comparison of the Green Valley color offset ($\Delta(U-V)$) of X-ray-selected AGNs and mass-matched inactive galaxies. The open histograms drawn with a solid black line show the distribution of $\Delta(U-V)$ for the AGNs, while shaded histograms correspond to the inactive galaxies. The statistical uncertainty in the distributions of the inactive galaxies is shown by the shading in the histograms—dark gray sections show the 1σ uncertainty, due to the scatter in the population as well as small number statistics, while the light gray sections show 2σ. The dashed line at $\Delta(U-V)=0$ is the location of the center of the Green Valley. The AGNs show very similar distributions to inactive galaxies, especially among the bluer star-forming population, but are underrepresented in the red sequence.

if the open histogram strongly or consistently deviates from the darkly shaded regions over a few or more bins in $\Delta(U-V)$. Note that systematic differences in the distributions due to cosmic variance are not represented in the uncertainties of these shaded histograms, though they can be important in small fields like GOODS and among the massive galaxies considered here. A comparison using both fields helps in this regard.

A quick examination shows that, in almost all redshift bins, there are very minor differences between AGNs and inactive galaxies. At the location of the GV, the AGNs are slightly more common than inactive galaxies, at the level of 1σ–1.5σ in five of six panels, but this difference is quite small and may be attributable to enhanced line emission or recombination continuum emission in AGNs, since nuclear activity can frequently produce extended, highly ionized, emission line regions. At about the same low level of significance, there is an enhancement of inactive galaxies over AGNs in the red sequence ($\Delta(U-V)$ in the range 0.2–0.6 mag). Perhaps the most significant difference between the two distributions is not near their peak, but is in the extreme blue wing, where AGNs are more common than inactive galaxies. This is likely due to the small fraction (a few percent) of AGNs which contain bright blue nuclear point sources which can dominate the integrated light of the system. These will have very blue colors for their stellar mass, a result of nuclear contamination in the optical and UV bands.

5. THE FIR-DERIVED SFRs OF X-RAY AGNs: COMPARISON TO INACTIVE GALAXIES

We now turn to a far better tracer of SF in galaxies: the FIR luminosity. Among massive galaxies, such as X-ray-selected AGN hosts, the FIR luminosity, an excellent tracer of the total dust-reprocessed UV light from star-forming regions, accounts for almost all the SF in the galaxy—the UV escape fractions in such galaxies is quite low and corrections for unreprocessed SF luminosity are at the level of a few percent (Pannella et al. 2009; Reddy et al. 2010; Whitaker et al. 2012).

The relative SF properties of AGN hosts and inactive galaxies can be understood more accurately by comparing their FIR luminosity distributions. Studies of the FIR SEDs of AGNs show that the contribution to L_{60} from dust emission heated by the active nucleus is low and generally negligible, except in a few cases of luminous AGNs in weakly SF galaxies (Netzer et al. 2007; Mullaney et al. 2011; Rosario et al. 2012). We can directly verify this for FIR-bright AGNs in the CDF fields, as done in Figure 5, where we compare measured L_{60} of AGNs detected in PACS with the predicted FIR luminosity derived from L_X based on model relationships of pure AGN-heated dust. These relationships, described in Rosario et al. (2012), have SED shapes covering the scatter found among local X-ray bright AGNs (Mullaney et al. 2011), while the nuclear X-ray luminosity is linked to the IR luminosity following the tight correlation of Gandhi et al. (2009). From the figure, it is clear that the AGN luminosities of most of the sources in our sample are too low to substantially affect the FIR luminosity.

Another simple test is to compare the IR colors of AGNs and inactive galaxies; if the FIR colors of AGNs are significantly warmer than inactive galaxies (i.e., with higher relative flux in bluer bands), then AGN heating may be responsible for a non-negligible fraction of L_{60}. In Figure 6, we plot the MIPS 24 μm to PACS 160 μm color against the PACS 100 μm to 160 μm color (both expressed as magnitudes) of PACS-detected AGNs and inactive galaxies. This plot may be directly compared to Figure 2 of Rosario et al. (2012), which studied the IR colors of sources in the COSMOS survey in similar fashion. The FIR color distributions of AGNs and inactive galaxies (histograms along the Y-axis in all panels) are formally indistinguishable, though, expectedly, AGN emission can influence the MIR, as

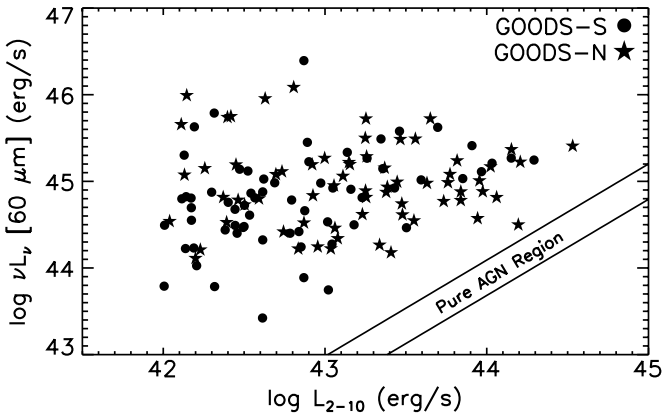

Figure 5. L_{60} plotted against the X-ray luminosity of the AGNs in both Chandra Deep Fields over the redshift range $0.5 < z < 2.0$. Different symbols are used to represent sources from the two different survey fields. The region between the two solid lines is where one may expect to find AGNs with negligible star-formation and FIR SEDs dominated by dust heated by the nucleus (see Section 5 and Mullaney et al. 2011). Essentially, all the AGNs have FIR luminosities well above the pure-AGN region. It is highly unlikely that AGN emission powers the FIR luminosity of these sources, even among those at the luminous end. Note that the apparent weak correlation between L_{2-10} and L_{60} is a consequence of Eddington bias and is not a real trend.

evidenced by the scatter of AGN points to bluer 24 to 160 μm colors. For essentially all of our PACS-detected AGNs, we can safely assume that L_{60} is a measure of the SFR.

Using FIR-based SFRs, AGNs share a similar scatter about the mass sequence ridgeline with inactive galaxies (lower panels of Figure 2), including a number of AGNs with GV colors that lie squarely on the mass sequence. We can evaluate this more rigorously by comparing ΔL_{60}, the offset of a galaxy from the Whitaker et al. (2012) mass sequence, for AGNs and mass-matched inactive galaxies (Figure 7). The known redshift and stellar mass of each object determines the corresponding MS value; then the Chary & Elbaz (2001) IR SED libraries and the relationship from Kennicutt (1998) are used to connect the MS to L_{60} (Section 2). In practice, the choice of comparing simple L_{60} distributions or ΔL_{60} distributions does not alter our basic result; we use the offset from the MS simply to scale out any stellar-mass dependent trend which would otherwise broaden the distributions. As for Figure 4, we use a bootstrap sampling procedure, randomly selecting a set of inactive galaxies matched to the AGNs in M_*, repeated a thousand times, to arrive at statistical uncertainties in the L_{60} distributions of the inactive galaxies. Dark/light gray regions show 1σ and 2σ uncertainties, respectively.

Unlike in $\Delta(U-V)$, there is a great deal of scatter in the inactive galaxy population in terms of FIR luminosity, as evidenced by 2σ uncertainties, which can span from zero to almost twice the number of AGNs at some values of ΔL_{60}. Despite this, we find that the AGN distributions are generally consistent with the inactive galaxy distributions at the 1σ–1.5σ level, i.e., the solid histograms lie within or close to the dark gray regions. There is a possible minor tendency for an excess of PACS-detected SF galaxies at or below the $\Delta L_{60}= 0$ line compared to AGNs in the GOODS-S panels at $z > 1$. However, this is not seen in GOODS-N and may just be due to cosmic variance. The broad consistency between the distributions implies that any differences in SF properties between AGN hosts and inactive galaxies that lie on or above the SF mass sequence are minor or non-existent, a result that is completely consistent with earlier work on the CDF X-ray-selected AGNs based on independent PEP and GOODS-*Herschel* data (Mullaney et al. 2012b; Santini et al. 2012b) or from studies from *Spitzer*/MIPS FIR surveys (e.g., Juneau et al. 2013). Star-forming AGN hosts are drawn from the general population of SF galaxies.

Galaxies with the greatest SF offset from the MS are known to be strong starbursts and frequently show highly disturbed morphologies consistent with being galaxy mergers (Wuyts et al. 2011). The ΔL_{60} distribution is dominated by galaxies close to the ridgeline of the MS and we have rather poor statistics for AGNs and galaxies at the highest ΔL_{60} ($\gtrsim$10), especially considering the substantial scatter shown in the distributions of inactive galaxies. Nevertheless, it is clear that AGNs are not strongly enhanced among starbursting galaxies, at least among the range of nuclear luminosities probed in the work.

There are, however, some clear differences between the populations of AGN hosts and inactive galaxies which come to light once we consider sources that are not detected in the PACS maps. These sources typically lie below the MS and include quenched galaxies and weakly star-forming galaxies

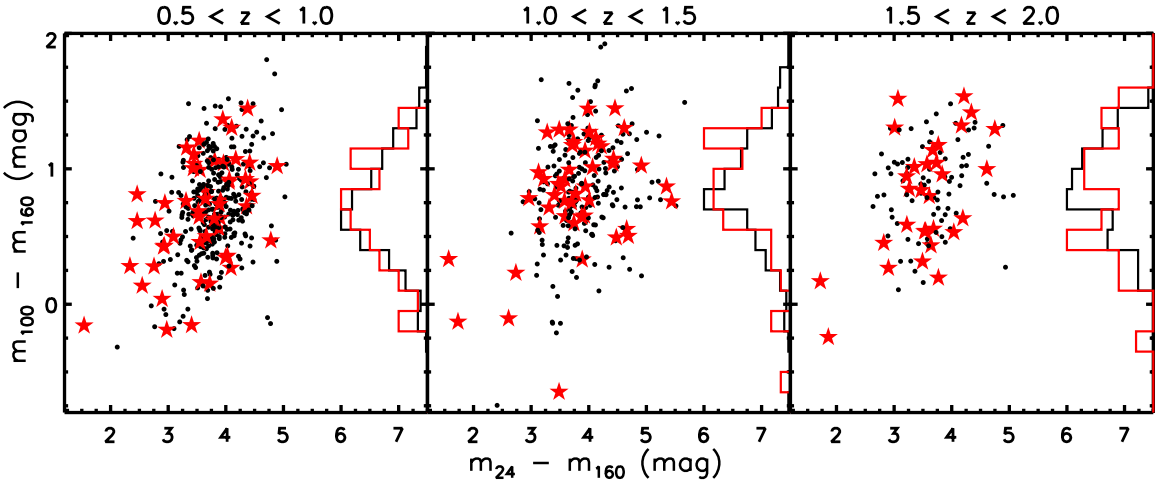

Figure 6. Infrared colors (in magnitudes) of PACS-detected AGNs (red star points) and inactive galaxies (small black points) from both GOODS fields combined. 24–160 μm (an MIR–FIR color) is plotted on the *X*-axis and 100–160 μm (an FIR–FIR color) is plotted on the *Y*-axis. Distributions of 100–160 μm colors are shown as histograms on the *Y*-axes, with red/black colors for AGNs/inactive galaxies, respectively. Both histograms are normalized to the same peak value. There is a small scatter of AGNs to low, blue MIR–FIR colors, due to the influence of AGN-heated dust on the 24 μm emission, but most AGNs lie in the area of the diagram occupied by inactive SF galaxies, implying that their FIR emission, if not the entire MIR-to-FIR SED, is dominated by SF-heated dust emission.

(A color version of this figure is available in the online journal.)

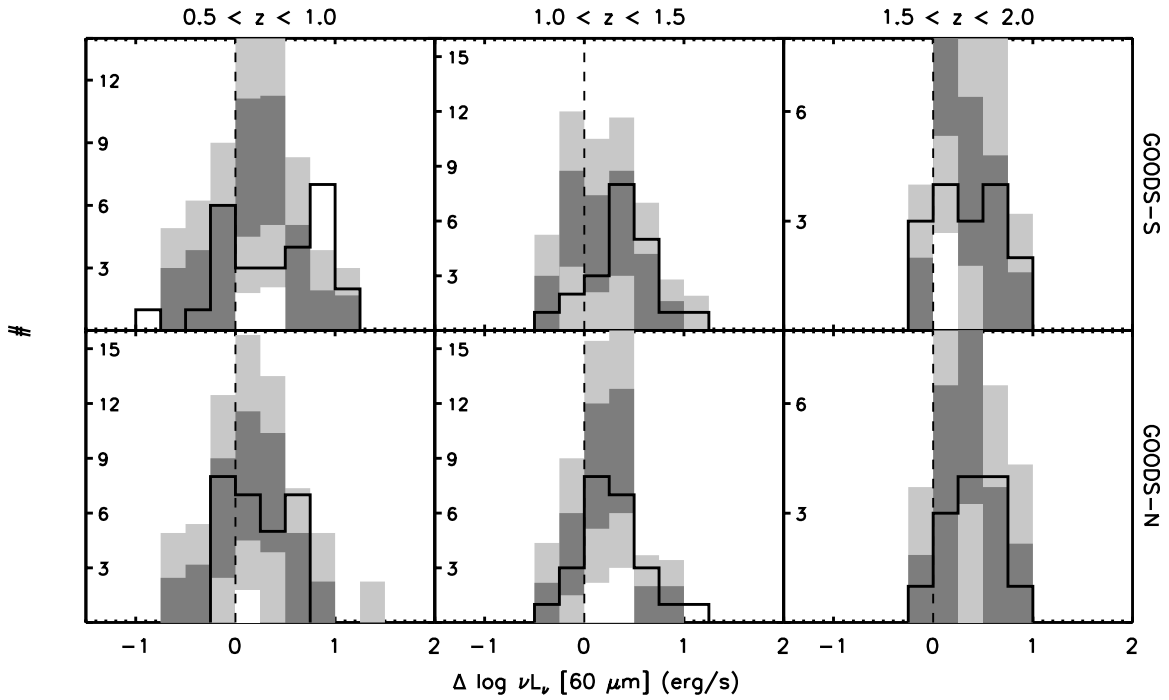

Figure 7. Comparison of the L_{60} offset (ΔL_{60}) of X-ray-selected AGNs and mass-matched inactive galaxies from the star formation mass sequence. The statistical uncertainty in the distributions of the inactive galaxies are shown by the shading in the histograms—dark gray sections show the 1σ uncertainty, due to the scatter in the population as well as small number statistics, while the light gray sections show 2σ. The dashed line at $\Delta L_{60} = 0$ corresponds to the center of the mass sequence. The AGNs show rather similar distributions to inactive galaxies.

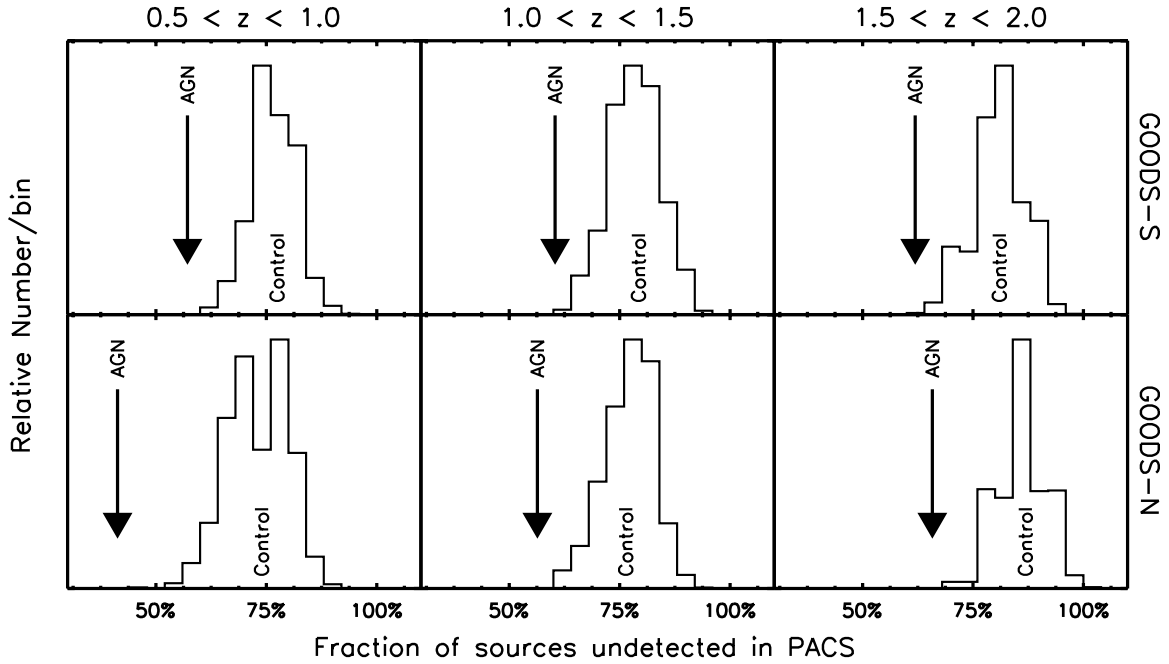

Figure 8. Histograms of the PACS non-detection fractions—the percentage of objects *not* detected in PEP+GH PACS maps—for 1000 realizations of the mass-matched comparison sample of inactive galaxies in the corresponding redshift bins. The median value of the histograms is shown by the location of the vertical label "Control." The non-detection fraction of X-ray AGNs in the same redshift bin is shown as a thick arrow for comparison. AGNs have a significantly higher chance of being detected in the deep *Herschel* data, which implies, given the depth of the PEP+GH maps, that they preferentially avoid weakly star-forming, quenching, or quiescent galaxies.

(i.e., normal SF galaxies that lie within the lower scatter of the MS). To understand this population, we compute the FIR "non-detection" fraction, f_{nd} which is the fraction of galaxies in each redshift bin that have no flux in both 100 and 160 μm PACS maps at the 3σ detection threshold of the catalogs. f_{nd} is a measure of the relative number of weakly star-forming or quiescent galaxies in a population.

In Figure 8, we plot the histogram of f_{nd} for inactive galaxies determined from the 1000 realizations of the mass-matching bootstrap procedure described above. The median non-detection fractions for this population are approximately 80%. This fraction is roughly independent of redshift despite the evolving luminosity limit of the PACS data, which reflects the fact that galaxies at $z \sim 2$ are typically more star-forming, and hence FIR

luminous, than at $z \sim 0.5$. In these insets, we show the value of f_{nd} for the AGNs in that redshift bin, a single number, using a thick downward-pointing arrow. It is immediately clear that the AGNs are always, at all redshifts and consistently in both fields, significantly more likely to be detected in PACS than the inactive galaxies. In other words, the fraction of quenching or quiescent galaxies hosting AGNs is considerably lower than similarly massive inactive galaxies, or, put differently, AGNs are more likely to be in star-forming galaxies around or above the MS. This result is in stark contrast to the notion that AGNs are preferentially in quenching systems. Controlling for the particular mass distribution of X-ray-selected AGN hosts, we show that, in fact, AGNs are *more likely* to be found in a galaxy that is forming stars, compared to one that is turning quiescent. This result strongly confirms the result from Santini et al. (2012b) that AGNs have higher FIR detection rates, which leads to the enhancement in mean SFR among AGNs compared to normal galaxies.

5.1. Biases and Tests

We have undertaken a series of tests to verify that this result is not due to possible biases in the data. Since the CDF sensitivity has a radial variation, the density of X-ray sources is higher in the central area of the field, while the comparison sample of background galaxies has a more uniform spatial distribution. Therefore, a possible bias may arise if the equivalent PACS coverage, which varies across the PEP+GH maps, differs between the AGNs and inactive sample. An examination of the PACS data coverage of AGNs and inactive galaxies shows that they are quite consistent; this is because the parts of the GOODS fields with strong PACS coverage gradients are restricted to the edges. We then repeated our analysis of FIR properties, while matching the AGNs and control galaxies to within a factor of 1.5 in PACS coverage, in addition to M_*. This severely limits the number of matched comparison galaxies for some of the AGNs in our sample, but does not change our main conclusions. Any differences in the spatial distribution of the AGNs and the comparison galaxy sample on the sky does not lead to a lower f_{nd} of the AGNs.

Another possible source of bias arises from the use of MIR (MIPS 24 μm) sources as priors during the photometric extraction of the PACS maps. In the small number of cases where a PACS source was a blend of multiple MIPS sources, FIR fluxes were decomposed using the 24 μm fluxes as weights. Since AGNs can be more MIR bright than inactive galaxies as a result of warm dust emission from the circumnuclear regions and torus, they could be assigned a stronger weight in blended sources, which can bias the FIR fluxes of AGNs, as a population, to inaccurately high values. To test this, we repeated our analysis but only including AGNs that had no neighboring 24 μm MIPS sources within a radius of 5″. The results were unchanged, implying that extraction biases, if present, have a negligible effect on the FIR photometry of X-ray-selected AGNs in the CDFs. We conclude that the low f_{nd} of AGNs is robust to systematic and data-related selection effects.

Finally, we consider the effects of AGN-heated dust emission on the FIR detection rates of AGNs. We have shown that the majority of these AGNs have luminosities that are too low to boost a significant fraction of weakly star-forming hosts into the PACS detectable regime—if this were the explanation of the low quenching fractions, PACS-detected AGNs in the CDFs should generally show very warm/blue FIR colors, which is not observed (Figure 6).

6. DISCUSSION: ARE AGN HOSTS A SPECIAL POPULATION OF GALAXIES?

We have undertaken a detailed analysis of the FIR luminosities and detection rates of low and moderate luminosity AGNs in the CDFs in the context of the population of inactive galaxies. Our key finding is the high FIR detection rates of AGNs, implying that they are significantly less likely to be hosted by galaxies undergoing a special phase of SF quenching, contrary to the results of earlier studies. This difference arises because, at the high masses of most AGN host galaxies, the UV-to-optical color is a poor proxy for SFRs, which has complicated earlier studies of the SF properties of AGNs based on the use of CMD or color–magnitude diagram. Our PACS detection rates for AGNs (∼50%) are higher than those reported in the *Spitzer*/MIPS 70 μm studies of (Juneau et al. 2013), but this is due to the significantly deeper PEP+GH data.

We also find that low and moderate luminosity X-ray AGNs have similar distributions of FIR luminosities as inactive SF galaxies, consistent with the notion that host galaxies of such AGNs are drawn from a population of mostly normal galaxies. In a study of $z \sim 0$ emission-line-selected AGNs from the Sloan Digital Sky Survey (SDSS), Pasquali et al. (2005) find evidence for a small (0.2 dex) enhancement in mean FIR luminosities over a control sample of normal SF galaxies, matched to the AGNs by multiple structural and photometric criteria. Given the difference in the AGN selection method and matching scheme, we are unable to make a detailed comment on the difference between our results and those from Pasquali et al. (2005). However, a small offset of the magnitude uncovered in that work may still be consistent with our findings, given the substantial uncertainties on the ΔL_{60} distributions in Figure 7 and the fact that the figure excludes some weakly star-forming galaxies. Alternatively, a study of UV-based SFRs of SDSS Type II AGNs by Salim et al. (2007) find that local "high-luminosity" AGNs, which are actually comparable in nuclear luminosity to the X-ray-selected AGNs from this work, lie on the local mass sequence, consistent with our result.

What could lead to the peculiar SF nature of AGN hosts? To answer this, we need to consider the relative timescales of bright AGN activity (i.e., detectable in X-ray surveys of high-redshift galaxies) and the modulation of SF on galaxy scales. It is highly unlikely that SMBHs accrete at a constantly high rate to maintain detectable AGN activity for a long period of time; typical constraints on the lifetime of a bright QSO phase suggest 10^{7-8} yr (Martini & Weinberg 2001; Hopkins et al. 2005; Shankar et al. 2010). Even during a period of substantial accretion, the luminous output of an AGN may change quite significantly. High-resolution simulations of SMBH accretion, both with and without the effects of feedback, suggest that the supply of gas to the accretion disk is not expected to flow in at a constant and steady pace (Hopkins & Quataert 2010; Novak et al. 2011). Therefore, the X-ray bright AGN population is probably a rather transient population among galaxies in the field.

On the other hand, SF on scales of the entire galaxy varies on timescales comparable to its dynamical time of around 10^8 yr. In addition, the FIR luminosity, arising mostly from dust heated by stars of a range of ages, is not a prompt measure of SFRs, but can average over timescales of tens to hundreds of Myr, especially in systems with fairly steady SF histories.

In light of this, we may consider two possible alternatives to explain our observations.

1. Some evolutionary models suggest that a major fraction of moderate luminosity AGNs arise in the aftermath of

a strong starburst, during which the SMBH also grows in a high accretion rate QSO-like phase (e.g., Ciotti & Ostriker 2007; Hopkins et al. 2008). A popular form of these models suggests that gas-rich major mergers modulate both starbursts and QSOs. The end product is a quenching post-starburst galaxy hosting a low-to-moderate luminosity AGN as the final amounts of gas fall intermittently into the SMBH. Within this scenario, the high PACS detection rates of AGN hosts may plausibly be ascribed to the gradual decline in dust heating by a post-starburst population, which serves as a fossil record of the coevolutionary phase which occurred within the last few 100 Myr. This picture would require a fine-tuning of the timescale between the peak of SF and the period over which low and moderate luminosity AGNs exist, in order to place the AGNs on the SF mass sequence with the same distribution of SSFRs as smoothly evolving inactive galaxies. It is also inconsistent with the observation that the [O II]-derived SFRs of moderate luminosity AGNs are comparable to normal star-forming galaxies (Silverman et al. 2009): emission line tracers are a more prompt measure of SF than the FIR and the starburst coevolution scenario would therefore predict a lower SF-powered line luminosity in AGNs than most comparable inactive galaxies. These observations disfavor the post-starburst/major merger picture as the driver for most low and moderate luminosity AGN activity.

There are suggestions that, among heavily obscured X-ray undetected AGNs at similar redshifts, the SFR is enhanced compared to the mass sequence (e.g., Juneau et al. 2013). One of the difficulties inherent in making the comparison of our work with such studies is the very different selection functions of X-ray-selected AGNs and, e.g., emission-line or MIR-selected AGNs. Taking a recent example, Juneau et al. (2013) find that the fraction of AGNs in a 70 μm detected sample of galaxies remains constant across SSFRs, consistent with our result, but only if one includes mass-excitation (MEx) selected objects undetected in the X-rays. However, the typical stellar mass of the MEx-selected AGNs in that study is significantly lower than the X-ray-detected AGNs, which automatically gives such objects a higher SSFR distribution in their FIR luminosity-limited sample (for a demonstration of this, notice the high SSFRs of low-mass AGNs in the lower panels of Figure 2). For a fair comparison between our work and studies of obscured AGNs, a full account of both redshift and stellar mass dependent selection effects needs to be taken. We aim to address obscured AGNs in future PEP+GH work following the methodology developed here.

2. A second view postulates that AGN hosts are simply drawn from a smoothly evolving population of massive star-forming galaxies. The connection here between SF and AGN activity is through the supply of cold gas needed for both, mediated through evolutionary processes that modulate SF in galaxy disks and carry gas to the nucleus for eventual accretion onto the SMBH. The lack of any clear relationship between nuclear and SF luminosities in low and moderate luminosity AGNs (Shao et al. 2010; Mullaney et al. 2012b; Rosario et al. 2012; Harrison et al. 2012a) argues against a prompt or synchronized connection between galaxy and black hole growth, favoring this scenario. The lower incidence of AGNs among weakly star-forming or quiescent galaxies is a consequence of the depleted supply of cold gas in such systems; SMBH activity in such galaxies is primarily in the form of a mechanically dominated low accretion rate mode, such as that found in most radio-loud AGNs (Churazov et al. 2005; Trump et al. 2011; Best & Heckman 2012).

If cold gas is necessary for fueling X-ray bright AGNs, then how do we reconcile this with the existence of such AGNs among genuinely quiescent galaxies, albeit at a low rate? This is indeed a puzzle, but is likely related to the fact that cold gas is not entirely absent in such systems. As many as 22% of nearby early-type galaxies harbor substantial molecular gas (Young et al. 2011) and some show clear SF (Crocker et al. 2011). Dusty disks with very low SF efficiencies are commonly seen in the circumnuclear regions of massive elliptical galaxies, while filamentary dust is frequent on larger scales (Lauer et al. 1995; Ferrarese et al. 2006). Kauffmann & Heckman (2009) have suggested that SMBH accretion rates in quiescent galaxies are set by the supply of gas from stellar mass loss. Indeed, only a small quantity of this gas needs to intermittently reach the nucleus to fuel such low-luminosity AGNs.

Existing surveys of large, complete samples of X-ray-selected AGNs suggest the existence of a universal accretion rate distribution for SMBHs, which is independent of the stellar mass of the host (Aird et al. 2012; Bongiorno et al. 2012). Our results can qualify these results by noting that the accretion rate distribution of AGN hosts do vary with SFRs—galaxies with ongoing SF are more likely to host a modestly accreting black hole than those that are quiescent. At lower stellar masses, both the gas supply and the SMBH mass drops, which is what possibly maintains the universal accretion rate distribution. However, the relative number of SF to quenched galaxies increases greatly with redshift—by $z \sim 2$, 70% of massive galaxies are widely forming stars (Fontana et al. 2009). Concurrent to this is an increase in the gas fractions of galaxies (Daddi et al. 2010; Tacconi et al. 2010, 2013). Therefore, the accretion rate distribution must change with redshift, both in normalization and shape, if, indeed, the supply of gas is what limits the time-averaged accretion rate of SMBHs. The form of this change would be a shift to a higher characteristic break in the accretion rate distribution, as more SMBHs of a given mass accrete from the more abundant cold gas supply at high redshifts. This is consistent with (Mullaney et al. 2012a) who show that average BH growth rates in mass-matched samples of galaxies indeed increase with redshift in line with their SFRs.

As a final point, we consider the effects of galaxy dust properties, which could alter the interpretation of our results. If AGNs are preferentially in galaxies with larger dust masses, this would lead to redder UV–optical colors over galaxies with smaller dust masses or lower average extinction. However, since dust is closely tied to gas, large dust masses would imply large gas reservoirs and, generally high SFRs, which only serves to underline our findings. The difficulty of using $U - V$ (or other similar colors) to understand SF properties in massive galaxies is compounded by the effects of dust extinction on these colors. For example, Cardamone et al. (2010) find that AGN hosts are common among galaxies where dust reddening has pushed colors from the star-forming blue cloud to the GV. This qualitatively agrees with our findings that AGNs are predominantly in star-forming galaxies. Cardamone et al. (2010) also suggest that AGN hosts in the red sequence and in star-forming galaxies have different accretion histories and feedback mechanisms. This may be true, but we maintain that, given the presence of molecular dusty gas even in genuinely quiescent

galaxies, cold gas accretion may still be responsible for some of the AGN activity on the red sequence.

7. SUMMARY

We characterize and study the star-forming properties of X-ray-selected active galaxies in the CDFs North and South using deep *Herschel*/PACS photometry at 70, 100, and 160 μm. Comparing the SFR distributions of X-ray-selected AGNs to those of inactive galaxies, we confirm that, after accounting for stellar mass selection effects, AGN hosts lie on the SF mass sequence out to $z \sim 2$, consistent with earlier studies (Mullaney et al. 2012b; Santini et al. 2012b). However, we also find that AGNs are much more likely to be hosted by a star-forming galaxy than a quiescent or quenching galaxy. This implies that AGNs are not preferentially found in galaxies that are undergoing a transformation from the blue cloud to the red sequence. Instead, AGN hosts are drawn primarily from the population of normal massive star-forming galaxies. This may be interpreted in a scenario where radiatively efficient AGNs, such as those selected by X-ray surveys, require a supply of cold gas to sustain such phases of SMBH accretion. Combined with results which show the lack of any clear correlation between global SF and nuclear activity in low and moderate luminosity AGNs (Shao et al. 2010; Mullaney et al. 2012b; Santini et al. 2012b; Rosario et al. 2012), our findings suggest that there may not exist any direct causal link between SMBH accretion and overall galaxy growth, but rather a more indirect relationship governed by the supply of gas, the fuel for both AGNs and SF.

PACS has been developed by a consortium of institutes led by MPE (Germany) and including UVIE (Austria); KU Leuven, CSL, IMEC (Belgium); CEA, LAM (France); MPIA (Germany); INAF-IFSI/OAA/OAP/OAT, LENS, SISSA (Italy); IAC (Spain). This development has been supported by the funding agencies BMVIT (Austria), ESA-PRODEX (Belgium), CEA/CNES (France), DLR (Germany), ASI/INAF (Italy), and CICYT/MCYT (Spain). F.B. acknowledges support from Financiamento Basal, CONICYT-Chile FONDECYT 1101024 and FONDAP-CATA 15010003, and Chandra X-ray Center grant SAO SP1-12007B (F.E.B.). J.R.M. acknowledges The Leverhulme Trust.

REFERENCES

Aird, J., Coil, A. L., Moustakas, J., et al. 2012, ApJ, 746, 90
Alexander, D. M., Bauer, F. E., Brandt, W. N., et al. 2003, AJ, 126, 539
Alexander, D. M., Swinbank, A. M., Smail, I., McDermid, R., & Nesvadba, N. P. H. 2010, MNRAS, 402, 2211
Bauer, F. E., Alexander, D. M., Brandt, W. N., et al. 2004, AJ, 128, 2048
Berta, S., Magnelli, B., Lutz, D., et al. 2010, A&A, 518, L30
Berta, S., Magnelli, B., Nordon, R., et al. 2011, A&A, 532, A49
Best, P. N., & Heckman, T. M. 2012, MNRAS, 421, 1569
Bongiorno, A., Merloni, A., Brusa, M., et al. 2012, MNRAS, 427, 3103
Brammer, G. B., van Dokkum, P. G., & Coppi, P. 2008, ApJ, 686, 1503
Brammer, G. B., Whitaker, K. E., van Dokkum, P. G., et al. 2009, ApJL, 706, L173
Brammer, G. B., Whitaker, K. E., van Dokkum, P. G., et al. 2011, ApJ, 739, 24
Bruzual, G., & Charlot, S. 2003, MNRAS, 344, 1000
Cano-Díaz, M., Maiolino, R., Marconi, A., et al. 2012, A&A, 537, L8
Cardamone, C. N., Urry, C. M., Schawinski, K., et al. 2010, ApJL, 721, L38
Chary, R., & Elbaz, D. 2001, ApJ, 556, 562
Cheung, E., Faber, S. M., Koo, D. C., et al. 2012, ApJ, 760, 131
Churazov, E., Sazonov, S., Sunyaev, R., et al. 2005, MNRAS, 363, L91
Ciotti, L., & Ostriker, J. P. 2007, ApJ, 665, 1038
Crocker, A. F., Bureau, M., Young, L. M., & Combes, F. 2011, MNRAS, 410, 1197
Daddi, E., Bournaud, F., Walter, F., et al. 2010, ApJ, 713, 686
Donley, J. L., Koekemoer, A. M., Brusa, M., et al. 2012, ApJ, 748, 142
Driver, S. P., Allen, P. D., Graham, A. W., et al. 2006, MNRAS, 368, 414
Elbaz, D., Daddi, E., Le Borgne, D., et al. 2007, A&A, 468, 33
Elbaz, D., Dickinson, M., Hwang, H. S., et al. 2011, A&A, 533, A119
Faber, S. M., Willmer, C. N. A., Wolf, C., et al. 2007, ApJ, 665, 265
Ferrarese, L., Côté, P., Jordán, A., et al. 2006, ApJS, 164, 334
Feruglio, C., Maiolino, R., Piconcelli, E., et al. 2010, A&A, 518, L155
Fioc, M., & Rocca-Volmerange, B. 1997, A&A, 326, 950
Fischer, J., Sturm, E., González-Alfonso, E., et al. 2010, A&A, 518, L41
Fontana, A., Santini, P., Grazian, A., et al. 2009, A&A, 501, 15
Franx, M., van Dokkum, P. G., Schreiber, N. M. F., et al. 2008, ApJ, 688, 770
Gandhi, P., Horst, H., Smette, A., et al. 2009, A&A, 502, 457
Giavalisco, M., Ferguson, H. C., Koekemoer, A. M., et al. 2004, ApJL, 600, L93
Gitti, M., Brighenti, F., & McNamara, B. R. 2012, AdAst, 2012
Grazian, A., Fontana, A., de Santis, C., et al. 2006, A&A, 449, 951
Greene, J. E., Zakamska, N. L., Ho, L. C., & Barth, A. J. 2011, ApJ, 732, 9
Harrison, C. M., Alexander, D. M., Mullaney, J. R., et al. 2012a, ApJL, 760, L15
Harrison, C. M., Alexander, D. M., Swinbank, A. M., et al. 2012b, MNRAS, 426, 1073
Holt, J., Tadhunter, C. N., & Morganti, R. 2008, MNRAS, 387, 639
Hopkins, P. F., Hernquist, L., Cox, T. J., & Kereš, D. 2008, ApJS, 175, 356
Hopkins, P. F., Hernquist, L., Martini, P., et al. 2005, ApJL, 625, L71
Hopkins, P. F., & Quataert, E. 2010, MNRAS, 407, 1529
Juneau, S., Dickinson, M., Bournaud, F., et al. 2013, ApJ, 764, 176
Kauffmann, G., & Heckman, T. M. 2009, MNRAS, 397, 135
Kauffmann, G., Heckman, T. M., De Lucia, G., et al. 2006, MNRAS, 367, 1394
Kennicutt, R. C., Jr. 1998, ARA&A, 36, 189
Lauer, T. R., Ajhar, E. A., Byun, Y.-I., et al. 1995, AJ, 110, 2622
Luo, B., Brandt, W. N., Xue, Y. Q., et al. 2010, ApJS, 187, 560
Lutz, D., Poglitsch, A., Altieri, B., et al. 2011, A&A, 532, A90
Magnelli, B., Elbaz, D., Chary, R. R., et al. 2009, A&A, 496, 57
Magnelli, B., Popesso, P., Berta, S., et al. 2013, A&A, 553, 132
Maiolino, R., Gallerani, S., Neri, R., et al. 2012, MNRAS, 425, L66
Martin, D. C., Wyder, T. K., Schiminovich, D., et al. 2007, ApJS, 173, 342
Martini, P., & Weinberg, D. H. 2001, ApJ, 547, 12
McNamara, B. R., & Nulsen, P. E. J. 2007, ARA&A, 45, 117
Mullaney, J. R., Alexander, D. M., Goulding, A. D., & Hickox, R. C. 2011, MNRAS, 414, 1082
Mullaney, J. R., Daddi, E., Béthermin, M., et al. 2012a, ApJL, 753, L30
Mullaney, J. R., Pannella, M., Daddi, E., et al. 2012b, MNRAS, 419, 95
Nandra, K., Georgakakis, A., Willmer, C. N. A., et al. 2007, ApJL, 660, L11
Netzer, H., Lutz, D., Schweitzer, M., et al. 2007, ApJ, 666, 806
Noeske, K. G., Weiner, B. J., Faber, S. M., et al. 2007, ApJL, 660, L43
Novak, G. S., Ostriker, J. P., & Ciotti, L. 2011, ApJ, 737, 26
Pannella, M., Carilli, C. L., Daddi, E., et al. 2009, ApJL, 698, L116
Pasquali, A., Kauffmann, G., & Heckman, T. M. 2005, MNRAS, 361, 1121
Reddy, N. A., Erb, D. K., Pettini, M., Steidel, C. C., & Shapley, A. E. 2010, ApJ, 712, 1070
Rodighiero, G., Daddi, E., Baronchelli, I., et al. 2011, ApJL, 739, L40
Rosario, D. J., Mozena, M., Wuyts, S., et al. 2013, ApJ, 763, 59
Rosario, D. J., Santini, P., Lutz, D., et al. 2012, A&A, 545, A45
Rupke, D. S. N., & Veilleux, S. 2011, ApJL, 729, L27
Salim, S., Rich, R. M., Charlot, S., et al. 2007, ApJS, 173, 267
Salmi, F., Daddi, E., Elbaz, D., et al. 2012, ApJL, 754, L14
Santini, P., Fontana, A., Grazian, A., et al. 2009, A&A, 504, 751
Santini, P., Fontana, A., Grazian, A., et al. 2012a, A&A, 538, A33
Santini, P., Rosario, D. J., Shao, L., et al. 2012b, A&A, 540, A109
Schawinski, K., Urry, C. M., Virani, S., et al. 2010, ApJ, 711, 284
Shankar, F., Weinberg, D. H., & Shen, Y. 2010, MNRAS, 406, 1959
Shao, L., Lutz, D., Nordon, R., et al. 2010, A&A, 518, L26
Silva, L., Maiolino, R., & Granato, G. L. 2004, MNRAS, 355, 973
Silverman, J. D., Lamareille, F., Maier, C., et al. 2009, ApJ, 696, 396
Sturm, E., González-Alfonso, E., Veilleux, S., et al. 2011, ApJL, 733, L16
Szokoly, G. P., Bergeron, J., Hasinger, G., et al. 2004, ApJS, 155, 271
Tacconi, L. J., Genzel, R., Neri, R., et al. 2010, Natur, 463, 781
Tacconi, L. J., Neri, R., Genzel, R., et al. 2013, ApJ, 768, 74
Taylor, E. N., Franx, M., van Dokkum, P. G., et al. 2009, ApJ, 694, 1171
Trump, J. R., Impey, C. D., Kelly, B. C., et al. 2011, ApJ, 733, 60
Whitaker, K. E., Labbé, I., van Dokkum, P. G., et al. 2011, ApJ, 735, 86
Whitaker, K. E., van Dokkum, P. G., Brammer, G., & Franx, M. 2012, ApJL, 754, L29
Willmer, C. N. A., Faber, S. M., Koo, D. C., et al. 2006, ApJ, 647, 853
Wuyts, S., Förster Schreiber, N. M., van der Wel, A., et al. 2011, ApJ, 742, 96
Wyder, T. K., Martin, D. C., Schiminovich, D., et al. 2007, ApJS, 173, 293
Xue, Y. Q., Brandt, W. N., Luo, B., et al. 2010, ApJ, 720, 368
Xue, Y. Q., Luo, B., Brandt, W. N., et al. 2011, ApJS, 195, 10
Young, L. M., Bureau, M., Davis, T. A., et al. 2011, MNRAS, 414, 940